

Residual Force Determines Surface Tension in Active Systems

Bal Krishan*

Department of Physical Sciences, Indian Institute of Science Education and Research, Mohali, Punjab, India

(Dated: December 9, 2025)

The mechanical tension at the interface of motility-induced phase separating active Brownian particles (ABPs) remains an open question. Here, we determine the surface tension by analyzing the spatial distribution of forces at the molecular level in a slab-confined system of ABPs exhibiting high and low density regions separated by a one-dimensional active interface. Unlike previous approaches that evaluate active and interaction stresses independently—often producing near-zero or negative surface tension—we show that on average, interaction forces act antagonistically to active propulsion, reducing the net force experienced by particles. By evaluating the work required to bring a particle to the interface using this total-force framework, we find a positive and physically consistent surface tension. These results reframe the mechanical interpretation of local stresses and provide a generalizable method for connecting microscopic force distributions to emergent interfacial properties in nonequilibrium systems.

Introduction - Inspired by living systems such as actin filaments propelled by molecular motors, bacterial colonies and birds flocks, active systems have become prototypical nonequilibrium condensed matter systems that exhibit novel properties such as dynamic clustering, swarming, large number fluctuations etc. and hold possibilities for the design of smart devices and materials at the micro-scales in future [1–5]. Due to constant energy expenditure at the level of individual constituents, these systems break detailed balance and operate far from thermodynamic equilibrium. In recent years, various experimental setups such as light-driven metal-coated Janus particles [6], bi-metallic particles suspended in a reaction medium where one of the metals acts as a catalyst [7] and more recently moving toys known as hex-bugs [8, 9] have been developed to understand the behaviour of active systems. See Ning *et al.* [10] for an extensive list. Due to slowing induced accumulation and many-body caging effects, active particles are known to phase separate in dense and dilute regions, a phenomena commonly known as motility induced phase separation (MIPS) [11–20]. MIPS has been observed in simulations of different models of active particles [11], in athermal systems [12], in systems without attractive interactions [13] and also in experiments [7]. Turci and Wilding [14] showed that even though activity lead to effective pairwise attraction among active particles interacting with repulsive only forces, multi-body effects play important role in MIPS. Nucleation events in MIPS can be controlled by seeding fixed obstacles inside the system [15]. Similarly, force absorbing walls can be used to accumulate particles and simulate the growing active interface [19–23].

A phase separated system possessing distinct high and low density regions naturally involves the formation of an interface region that separates the two regions with different densities. In a single component equilibrium fluid undergoing phase separation, density heterogeneity

across the interface leads to inhomogeneous distribution of molecular forces in the interface region which are responsible for emergence of surface tension at the interface [24]. While connection between molecular forces and surface tension is extensively studied for interfaces in passive systems [24–26], the existing literature lacks an in depth study of forces in the interface region for active systems. Bialke *et al.* [21] found large negative values for the surface tension of active interface formed by active Brownian particles (ABPs) interacting with repulsive only Weeks-Chandler-Anderson (WCA) potential in two dimensions. Since then, several attempts have been made to determine the surface tension for MIPS phase separating interface for repulsive ABPs. Using similar approach, Patch *et al.*[20] also found large negative values of surface tension while using a different way to evaluate the pressure due to active force. Omar *et al.* [22], however, argued that due to its anisotropic nature, the swim stress is not a true stress and should more appropriately be understood as a force density. Using simulations of ABPs in three dimensions, they found that when swim stress is excluded, near zero values of surface tension are obtained and showed that inclusion of swim stress results in negative values of surface tension. See Li *et al.*[27] for an excellent overview of previous works, wherein a more generalized relation for surface tension of non-equilibrium interface is also derived which results in large positive values.

Most of the above mentioned works are concerned with simulations of ABPs in a periodic box, often elongated, where MIPS leads to formation of clusters. Due to elongated shape of the box, most clusters merge together to form one large cluster that spans the shorter length of the box leading to two interfaces parallel to the shorter length. Our approach, to analyze the one dimensional active interface between the higher and lower density regions formed using a rigid confinement along the longer length of the box, has been successful in gaining insights into the finite size scaling behaviour of the active interface, though only at large activity values [23]. An important distinction between these two kinds of ac-

* ph19051@iisermohali.ac.in

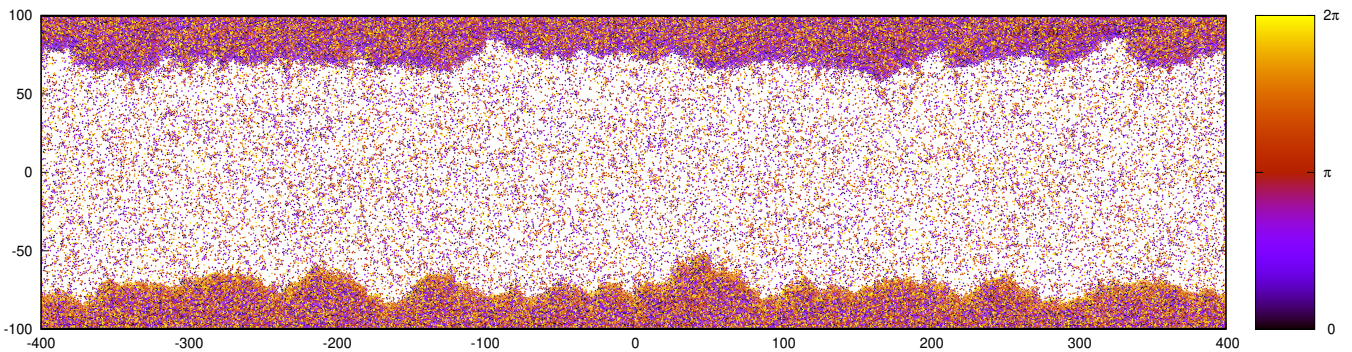


FIG. 1. Steady state snapshot for a system of 100172 ABPs confined in a box of size 800×200 showing active interface in the steady state ($t = 250$) at a large activity value ($Pe = 125$). Orientation of particles is depicted in colour. Higher concentration of violet in the upper region and orange in the lower region shows preferential sorting of particle orientations by the confining walls.

tive interfaces, one formed by ABPs in an elongated periodic box and the other by confined ABPs is that in the first case droplet formation and mergers dominate the dynamics of clustering, processes which in the absence of restriction of an elongated box, leads to curved interfaces such as those produced by the Eden model [28] while, in latter case, presence of confinement results in sorting and trapping of particles near the confinement and forms one dimensional interfaces. The present work extends our understanding of behaviour of one dimensional active interfaces formed due to confinement at more activity values than previously known. We do this by determining the average spatial distributions of forces experienced by particles at the molecular level. We find that magnitude of pairwise repulsive force increases with increasing density and effectively acts as a response to the active force which increases significantly in the denser region due to particle sorting induced by the presence of confinement. Average forces are found to be non-zero only along the direction normal to the confinement, as expected due to symmetry. At the interface, active force is found to exhibit a slightly larger magnitude as compared to the interaction force which stabilizes the interface. We use the knowledge of spatial distributions to determine the mechanical surface tension at the active interface by evaluating the amount of work required to bring a particle at the interface.

Methods and Results - Simulation setup used in this work is exactly the same that I have used earlier to determine the finite size scaling and universality classes of the growing active interface formed due to confinement [23]. Despite the resemblance, the present work addresses a different question and makes use of unrelated analysis. Our system consists of N active Brownian particles confined between two rigidly held parallel walls moving in two dimensions whose dynamics is governed by the set of coupled overdamped Langevin equations,

$$\begin{aligned} \dot{\mathbf{r}}_i &= D\beta(\mathbf{F}_i^{int}(r_{ij}) + \mathbf{F}_i^{wall}(r_{ij}) + \hat{v}_i v_p) + \sqrt{2D}\boldsymbol{\eta}_r \\ \dot{\theta}_i &= \sqrt{2D_r}\eta_\theta \end{aligned} \quad (1)$$

Here, position and orientation coordinates of particles are represented by $\{\mathbf{r}_i, \theta_i\}$, v_p denotes the magnitude of active force and its direction is given by the unit vector $\hat{v}_i = (\cos \theta_i, \sin \theta_i)$. Translational and rotational diffusion coefficients are written as D and D_r respectively which are taken to be related as $D_r = 3D/\sigma^2$ where σ represents the diameter of the particles. Walls used in our simulations are made up of particles of same size as ABPs which are rigidly held at their positions. Inter-particle interaction force $\mathbf{F}_i^{int}(r_{ij})$ with $r_{ij} = |\mathbf{r}_i - \mathbf{r}_j|$ and the wall forces $\mathbf{F}_i^{wall}(r_{ij})$, are both obtained using the WCA potential[29],

$$U(r) = \begin{cases} 4\epsilon[(\frac{\sigma}{r})^{12} - (\frac{\sigma}{r})^6] + \epsilon & \text{if } r < 2^{1/6}\sigma \\ 0 & \text{otherwise} \end{cases} \quad (2)$$

We take D , σ and $\epsilon = 1/\beta$ to be one. Dimensionless Peclet number $Pe = v_p\sigma/D$ governs the magnitude of self propulsion force v_p and $\{\eta_i\}$ are Gaussian white noise variables with

$$\langle \eta_i(t) \rangle = 0 \quad \text{and} \quad \langle \eta_i(t)\eta_j(t') \rangle = \delta_{ij}\delta(t-t') \quad (3)$$

Above system of ABPs with periodic boundary conditions (in absence of walls) was first studied by Redner *et al.* [13] who determined the MIPS phase diagram of the system. We use a set of confining walls parallel to x -axis while retaining periodic boundaries in the other direction to obtain access to the active interface. The confinement leads to preferential sorting of particle orientations with the particles pointing upwards (downwards) getting accumulated at the upper (lower) confinement as shown in Fig. 1.

To determine the spatial distribution of molecular forces, we carried out simulations for $N = 100172$ ABPs confined between parallel walls in a box of size 800×200 for different Pe values as discussed before. Time step is taken to be 1.0×10^{-5} for $Pe \geq 100$ and 2.0×10^{-5} for smaller Pe values and 50 uniformly spaced snapshots of the system are stored for every unit of time elapsed. Our earlier study [23] of this system showed that for a

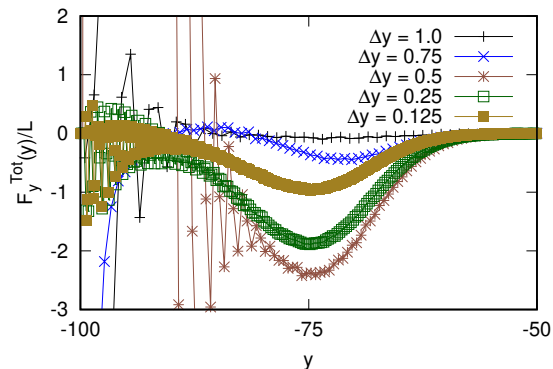


FIG. 2. Total force per unit length along the y -direction for different thickness Δy of the coarse-graining strip for $Pe = 125$. Total force per unit length in the region of interface increases as Δy increase from 0 to $\sigma/2$ because a larger Δy implies more particles contribute to the sum of forces. Beyond $\Delta y > \sigma/2$, though even larger number of particles contribute to the sum of forces, $F_y^{Tot}(y)$ is found to decrease due to the onset of bulk effects.

high activity value $Pe = 125$, mean height of the interface and mean orientation coordinate probabilities both achieve stationary values for $t \gg 7.5$. Numerical results on steady state spatial distribution of molecular forces, presented below are obtained by performing extensive time averaging for 5000 uniformly spaced snapshots in the range $100 < t \leq 200$ and ensemble averaged over five or more systems.

As can be seen in Fig. 1, mean particle densities along the coordinate parallel to the interface (x -axis) are symmetric and uniform due to presence of the confinement. On the other hand, mean density profile along y -axis is inhomogeneous. Symmetry along the coordinate parallel to the interface (x -axis) similarly affects the average distribution of molecular forces across the system. We therefore examine average molecular forces, as a function of the y -coordinate only. This is achieved by dividing the system into smaller sub boxes that span the entire length along x -direction and a thickness Δy along y -direction. The interaction and swim forces on all particles in each sub box are added together and divided by the length of the confining substrate to obtain total force per unit length \mathbf{F}^{Tot}/L ,

$$\frac{\mathbf{F}^{Tot}(y)}{L} = \frac{\sum_i (\mathbf{F}_i^{Act}(y) + \mathbf{F}_i^{Int}(y))}{L} \quad (4)$$

where L is the length of the confining substrate and F_i^{Act} and F_i^{Int} are respectively the active and interaction force on i^{th} particle and summation is over all particles in the strip at y . Since normal to length L points along y -direction, the x and y components of $\mathbf{F}^{Tot}(y)/L$ represent components of the mechanical stress tensor σ_{xy} and σ_{yy} respectively for our two dimensional system. As expected due to symmetry, the x -component, $F_x^{Tot}(y)/L = \sigma_{xy}$ is found to be near zero on average which is shown later. Interestingly, at the interface, total

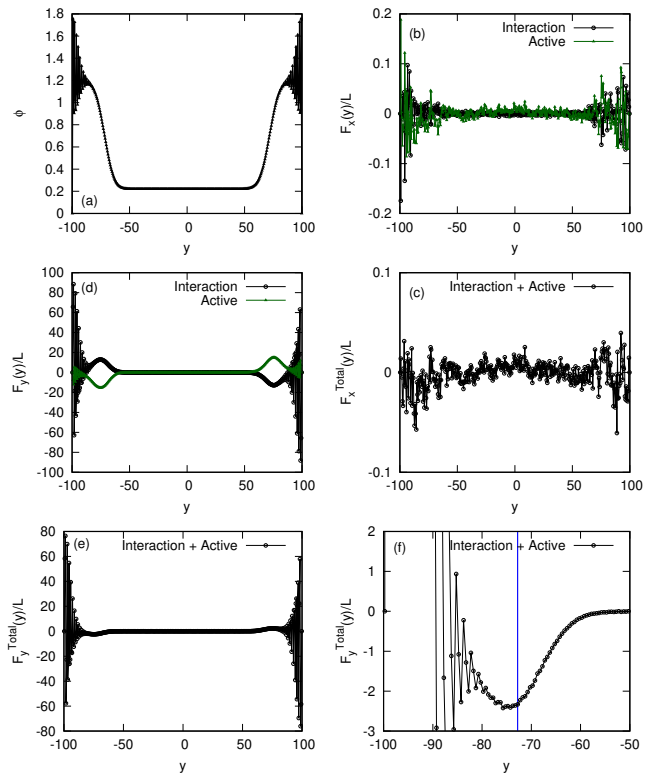


FIG. 3. For a system of confined ABPs with $Pe = 125$, (a) average packing fraction as a function of the y -coordinate. (b) Average active and interaction force per unit length parallel to interface (x -axis). (c) Total force per unit length in the direction parallel to the interface. (d) Average active and interaction force per unit length in the direction normal to the interface (y -axis). (e) Total force per unit length in the direction normal to the interface. (f) Total force per unit length in the direction normal to the interface zoomed in on the interfacial region with blue vertical line representing the average position of the interface. Data points are joined with lines.

force per unit length in the direction normal to the interface $F_y^{Tot}(y)/L$, shown in Fig. 2, is found to depend non-monotonically on the thickness Δy of the coarse graining strip. For an arbitrary strip, as Δy is increased from zero, total force per unit length increases because for a larger Δy , more particles contribute to $\mathbf{F}^{Tot}(y)$ due to decrease in number of strips. However, beyond $\Delta y = \sigma/2$, where σ is the particle diameter, a further increase in Δy results in decrease in $\mathbf{F}^{Tot}(y)$ due to the onset of bulk effects. A maximum value of force per unit length is thus obtained for $\Delta y = \sigma/2$. For this reason, we choose $\Delta y = \sigma/2$ to obtain spatial distribution of average active and interaction forces. Phenomena at the interface such as surface tension are manifestations of forces at the molecular level and it only seems natural to probe them at microscopic scales. It is worth pointing out that we have not accounted for frictional forces for the simple reason that they are isotropically distributed in the lower density phase due to randomized particle motion and are

negligible in the high density region where particle velocities are very small.

Fig. 3 shows the packing fraction and average force per unit length using the above mentioned coarse-graining procedure, for $Pe = 125$ where a reliable estimation of interface boundary is possible [23]. Packing fraction of the system, shown in Fig. 3 (a), changes rapidly across the interface and exhibits oscillatory behaviour in the dense phase due to sub-microscopic lengthscale used while evaluating averages. Parallel to the interface, along x -direction, both interaction and swim forces exhibit negligible magnitude and small fluctuations about zero which can be seen in Fig. 3 (b) and (c). In the direction normal to the interface, both active force and interaction force exhibit extremum values near the position of the interface and oscillatory behaviour near the confinement which is shown in Fig. 3 (d) where it can also be seen that in the denser phase, the magnitude of the interparticle repulsion forces far exceeds the magnitude of the swim force. The oscillatory behaviour in denser region is expected for the sub-microscopic thickness of the coarse graining strip such as $\Delta y = \sigma/2$ that we have chosen. Sum of the two forces in the direction normal to the interface is shown in Fig. 3 (e) with a closer look at the interfacial region in Fig. 3 (f) where the blue vertical line which represents the mean position of the interface, can be observed to be near the extremum of total force per unit length. It can also be seen from Fig. 3 (f) that at the interface, the magnitude of active force is larger than the magnitude of interaction force which leads to the formation of a stable interface.

Previous approaches to compute surface tension in active interfaces resulted in large negative values [20, 21], with the use of active pressure, which includes contributions from the active force. Excluding active contributions, as suggested by Omar *et al.* [22], leads to near-zero surface tension because interaction stresses in tangential and normal directions approximately balance. This limitation reflects the inadequacy of evaluating stresses from individual forces alone: in the bulk, interaction and active forces partially cancel, reducing the net force on particles away from boundaries.

To avoid unphysical results arising from conventional stress-tensor integration, we compute surface tension mechanically as the work required to bring a particle from the bulk to the interface. Because the total force is significant only in the direction normal to the interface (y -direction), the surface tension can be written as,

$$\gamma = \int_0^{y_i} F_y^{Tot}(y) dy \quad (5)$$

where $F_y^{Tot}(y)$ is the total normal force on a particle of unit diameter and y_i represents the mean interface position. The particle is transported from the low-density region toward the interface, and the corresponding work effectively captures the interfacial force imbalance without invoking the stress tensor. This approach is consistent with the general thermodynamic interpretation of surface tension as the reversible work required to create

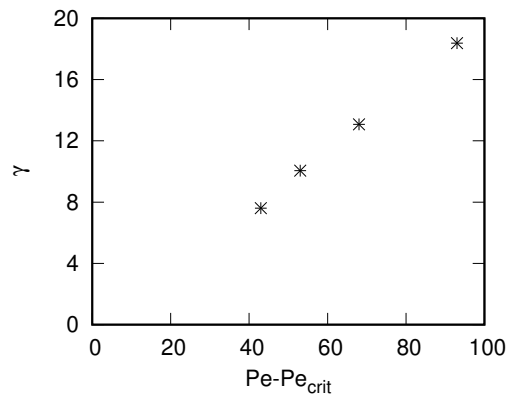


FIG. 4. Surface tension of the active interface obtained by evaluating the amount of work required to bring a particle from bulk region to the interface plotted as a function of $Pe - Pe_{crit}$ where $Pe_{crit} \approx 32$ is the critical value of swim force.

or sustain an interface, while providing a mechanically transparent measure of the interfacial energetics in systems where local stress fields are not well defined. Notably, tangential force components vanish at a flat interface due to symmetry.

The resulting surface tension values, shown in Fig. 4 for $75 \leq Pe \leq 125$ are of order ~ 10 (in units of ϵ/σ^2), in clear contrast to the near-zero or negative values reported from Kirkwood–Buff formulations [20–22]. Moreover, the computed tension shows a systematic dependence on $Pe - Pe_{crit}$, suggesting a progressive strengthening of interfacial cohesion with increasing activity, although additional data, particularly at lower Pe , are needed to fully characterize this relationship. See Appendix A for details on methods used to determine Pe_{crit} .

Discussion - We have determined the mechanical surface tension of a one-dimensional active interface in a system of confined active Brownian particles (ABPs) by analyzing the spatial distribution of microscopic forces. By coarse-graining over a sub-microscopic length scale normal to the interface, we show that the mean force per unit length at the interface is non-zero only in the normal direction, despite rapid fluctuations at the particle level. Crucially, the active/swim forces are slightly larger than the interaction forces that stabilize the interface, but the net effect of their antagonistic interplay determines the emergent mechanical stress, providing a physically consistent, positive value for surface tension. This framework contrasts with previous approaches that evaluate active and interaction contributions independently or rely on equilibrium assumptions such as the capillary wave theory. Our method yields a true non-equilibrium surface tension, independent of equilibrium-based approximations, and highlights the importance of considering forces collectively rather than individually.

Because the results are obtained via extensive averaging, they are equivalent to the macroscopic limit where interface fluctuations are small compared to its

length, making them amenable to experimental validation. While we have focused on the two dominant forces in ABPs, further refinements are necessary to capture subtler effects such as rotational friction in dense regions or alignment interactions in chiral or Vicsek-like active particles, which may influence force distributions and surface tension. Overall, this work provides a generalizable principle for understanding mechanics in active matter: the effective mechanical stress is set by the residual force from opposing active and interaction contributions, offering a unified perspective on how microscopic interactions give rise to emergent non-equilibrium interfacial properties.

ACKNOWLEDGEMENT

I would like to thank Abhishek Chaudhuri for various discussions. For compute resources, I acknowledge 'National Supercomputing Mission' for access to 'PARAM SMRITI' at NABI, Mohali which is implemented by C-DAC and HPC Facility at IISER Mohali. Financial support from CSIR-HRDG, India via grant no. (09/947(0248)/2019-EMR-I) is duly acknowledged.

Appendix A: MIPS in Presence of Confinement

From numerical simulations of 12484 confined ABPs in a box of size 100×200 for varying Pe values, I determined the density bifurcation diagram and the Binder cumulant by averaging over 5000 uniformly spaced snapshots in the range $100 < t \leq 200$. We take $dt = 2.0 \times 10^{-5}$. The nonlinear least square method is used to fit the average packing fraction distributions $P(\phi)$ using a uni-model/bi-model Gaussian distribution and determine the mean densities in each phase which are shown in Fig. 5 (a). This process enables us to bracket the MIPS critical point for the system of confined ABPs in the range $25 < Pe < 40$ where fitting becomes unreliable due to large unavoidable errors in estimating the parameter val-

ues. The bifurcation diagram of densities shown in Fig. 5 (a) is qualitatively similar to that of ABPs in a periodic box. See Redner *et al.* [13] for the corresponding bifurcation diagram for ABPs in a box with periodic boundary conditions. Following Siebert *et al.* [30], I evaluate the Binder cumulant U_L , to locate the MIPS critical point which is defined as,

$$U_L = \langle m_L^2 \rangle^2 / \langle m_L^4 \rangle \quad (\text{A1})$$

where $m_L = \phi_L - \langle \phi \rangle$ represents the order parameter, the density fluctuations. Here, ϕ_L is the packing fraction in a square sub-box of side L and $\langle \phi \rangle$ denotes mean packing fraction. For different activity values, the Binder cumulant U_L is shown in Fig. 5 (b) for varying sub-box size L and is evaluated by first determining the packing fraction distribution for each L value. Two observations regarding the observed Binder cumulant are in order: (1) while U_L vs Pe curves are not exactly smooth, they are surprising close to $1/3$, as expected from a uni-model Gaussian distribution near the critical point and, (2) U_L exhibits near L independence and crossover for different L values at the critical activity value, $Pe_{crit} \approx 32$.

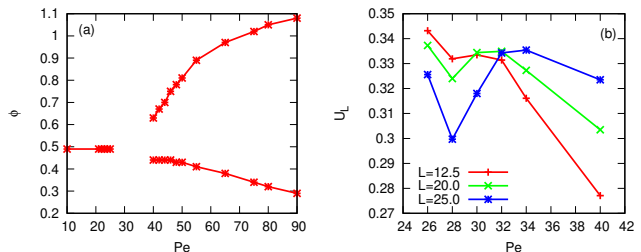


FIG. 5. (a) The density bifurcation diagram obtained using nonlinear least square fitting of the packing fraction. The region between $25 < Pe < 40$ has no points as the fitting become unreliable in this region. (b) Binder cumulant for varying sub box size L is found to exhibit L independence and crossover at $Pe = 32$. Data points are joined by line segments which serve as a guide to the eye.

-
- [1] T. Vicsek, A. Czirók, E. Ben-Jacob, I. Cohen, and O. Shochet, *Phys. Rev. Lett.* **75**, 1226 (1995).
 - [2] M. C. Marchetti, J. F. Joanny, S. Ramaswamy, T. B. Liverpool, J. Prost, M. Rao, and R. A. Simha, *Rev. Mod. Phys.* **85**, 1143 (2013).
 - [3] J. Toner and Y. Tu, *Phys. Rev. Lett.* **75**, 4326 (1995).
 - [4] J. Toner and Y. Tu, *Phys. Rev. E* **58**, 4828 (1998).
 - [5] J. Joanny and J. Prost, *HFSP Journal* **3**, 94 (2009).
 - [6] H.-R. Jiang, N. Yoshinaga, and M. Sano, *Physical Review Letters* **105** (2010), 10.1103/physrevlett.105.268302.
 - [7] I. Theurkauff, C. Cottin-Bizonne, J. Palacci, C. Ybert, and L. Bocquet, *Phys. Rev. Lett.* **108**, 268303 (2012).
 - [8] A. Deblais, T. Barois, T. Guerin, P. H. Delville, R. Vaudaine, J. S. Lintuvuori, J. F. Boudet, J. C. Baret, and H. Kellay, *Phys. Rev. Lett.* **120**, 188002 (2018).
 - [9] A. Barona Balda, A. Argun, A. Callegari, and G. Volpe, *American Journal of Physics* **92**, 847 (2024), <https://pubs.aip.org/aapt/ajp/article-pdf/92/11/847/20213521/847.1.5.0125111.pdf>.
 - [10] L. Ning, H. Zhu, J. Yang, Q. Zhang, P. Liu, R. Ni, and N. Zheng, *National Science Open* **3** (2024), <https://doi.org/10.1360/nso/20240005>.
 - [11] M. E. Cates and J. Tailleur, *Annual Review of Condensed Matter Physics* **6**, 219 (2015), <https://doi.org/10.1146/annurev-conmatphys-031214->

- 014710.
- [12] Y. Fily and M. C. Marchetti, *Phys. Rev. Lett.* **108**, 235702 (2012).
- [13] G. S. Redner, M. F. Hagan, and A. Baskaran, *Phys. Rev. Lett.* **110**, 055701 (2013).
- [14] F. Turci and N. B. Wilding, *Phys. Rev. Lett.* **126**, 038002 (2021).
- [15] C. Reichhardt and C. J. Olson Reichhardt, *Soft Matter* **10**, 7502 (2014).
- [16] C. Maggi, M. Paoluzzi, A. Crisanti, E. Zaccarelli, and N. Gnan, *Soft Matter* **17**, 3807 (2021).
- [17] B. Partridge and C. F. Lee, *Phys. Rev. Lett.* **123**, 068002 (2019).
- [18] A. K. Omar, K. Klymko, T. GrandPre, and P. L. Geissler, *Phys. Rev. Lett.* **126**, 188002 (2021).
- [19] C. F. Lee, *Soft Matter* **13**, 376 (2017).
- [20] A. Patch, D. M. Sussman, D. Yllanes, and M. C. Marchetti, *Soft Matter* **14**, 7435 (2018).
- [21] J. Bialké, J. T. Siebert, H. Löwen, and T. Speck, *Phys. Rev. Lett.* **115**, 098301 (2015).
- [22] A. K. Omar, Z.-G. Wang, and J. F. Brady, *Phys. Rev. E* **101**, 012604 (2020).
- [23] B. Krishan, *Europhysics Letters* **150**, 37003 (2025).
- [24] J. Rowlinson and B. Widom, *Molecular Theory of Capillarity*, Dover books on chemistry (Dover Publications, 2002).
- [25] M. V. Berry, *Physics Education* **6**, 79 (1971).
- [26] E. V. Grekov, *European Journal of Physics* **42**, 055104 (2021).
- [27] L. Li, Z. Sun, and M. Yang, *Proceedings of the National Academy of Sciences* **122**, e2505010122 (2025).
- [28] M. Eden *et al.*, in *Proc. 4th Berkeley Sympos. Math. Statist. and Prob.*, Vol. 4 (1961) pp. 223–239.
- [29] J. D. Weeks, D. Chandler, and H. C. Andersen, *The Journal of Chemical Physics* **54**, 5237 (1971), https://pubs.aip.org/aip/jcp/article-pdf/54/12/5237/10967422/5237_1_online.pdf.
- [30] J. T. Siebert, F. Dittrich, F. Schmid, K. Binder, T. Speck, and P. Virnau, *Phys. Rev. E* **98**, 030601 (2018).